JOC The Journal of Organic Chemistry

Article

pubs.acs.org/joc

The K-Region in Pyrenes as a Key Position to Activate Aggregation-Induced Emission: Effects of Introducing Highly Twisted *N,N*-Dimethylamines

Shunsuke Sasaki,*[,†] Satoshi Suzuki,[‡] Kazunobu Igawa,[§] Keiji Morokuma,[‡] and Gen-ichi Konishi*[,†]

[†]Department of Organic and Polymeric Materials, Tokyo Institute of Technology, Tokyo 152-8552, Japan

[‡]Fukui Institute for Fundamental Chemistry, Kyoto University, Kyoto 606-8103, Japan

[§]Institute for Materials Chemistry and Engineering and Department of Molecular and Material Sciences, Kyushu University, Fukuoka 816-8580, Japan

Supporting Information

ABSTRACT: A new design strategy to activate aggregation-induced emission (AIE) in pyrene chromophores is reported. In a previous report, we demonstrated that highly twisted *N,N*-dialkylamines of anthracene and naphthalene induce drastic AIE when these donors are introduced at appropriate positions to stabilize the S_1/S_0 minimum energy conical intersection (MECI). In the present study, this design strategy was applied to pyrene: the introduction of *N,N*-dimethylamine substituents at the 4,5-positions of pyrene, the so-called K-region, are likely to stabilize MECIs. To examine this hypothesis, four novel pyrene derivatives, which contain highly twisted *N,N*-dimethylamino groups at the 4- (**4-Py**), 4,5- (**4,5-Py**), 1- (**1-Py**), or 1,6-positions (**1,6-Py**) were tested. The nonradiative transitions of **4,5-Py** are highly efficient (k_{nr} = 57.1 × 10^7 s^{-1}), so that its fluorescence quantum yield in acetonitrile decreases to Φ_{fl} = 0.04. The solid-state fluorescence of **4,5-Py** is efficient (Φ_{fl} = 0.49). In contrast, **1,6-Py** features strong fluorescence (Φ_{fl} = 0.48) with a slow nonradiative transition (k_{nr} = 11.0 × 10^7 s^{-1}) that is subject to severe quenching (Φ_{fl} = 0.03) in the solid state. These results underline that the chemistry of the pyrene K-region is intriguing, both from a photophysical perspective and with respect to materials science.

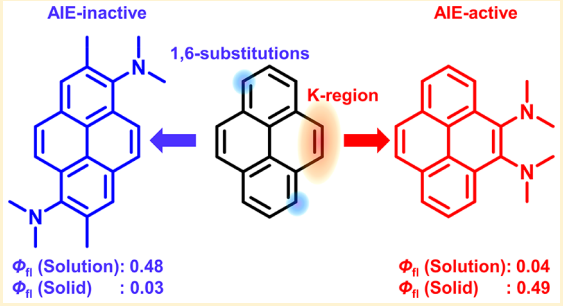

INTRODUCTION

Pyrene is one of the most attractive polycyclic aromatic hydrocarbons (PAHs) for the development of novel π-systems with photophysical, photochemical, and electronic functionalities. The most outstanding feature of pyrene is the versatility of its structural modifications: in addition to its four main points of reactivity, i.e., the 1-, 3-, 6- and 8-positions, recent studies revealed that the K-region (4-, 5-, 9-, and 10-positions), as well as the unreactive 2- and 7-positions are available for further modifications.[1,2] This advantage has been used to create various large molecular systems such as metal−organic frameworks,[3] cyclic compounds,[4] dendrimers,[5] and liquid crystals.[6] In addition, the large π-plane of pyrene often provides superior photoluminescence and electronic properties, which is reflected in numerous applications such as fluorescence probes,[7] organic field-effect transistors,[8] and organic light-emitting diodes.[9] Thus, pyrene has frequently been employed as a building block for larger π- and supramolecular systems. However, few studies have focused on the substitution effects of electron donors (D) or acceptors (A) in order to induce photophysical functionality.

Recently, our group has comprehensively investigated the effects of various asymmetric substitution patterns at the 1-, 3-, 6,- and 8-positions of pyrene, and observed regioisomer-specific photophysical properties in these pyrene chromophores.[10] Moreover, Yamato et al. have examined photophysical functionality derived from the regioselective substitution at the 1,3- and 6,8-positions.[11] In contrast to these recent advances at the 1-, 3-, 6,- and 8-positions, pyrene derivatives substituted at the 4-, 5-, 9-, and 10-positions (K-region) have been employed predominantly as synthetic intermediates for fused π-systems.[12−14] Accordingly, only few studies have examined the effects of substitution at the 4-, 5-, 9-, and 10-position on the photophysical functionality of pyrenes.[15,16] Even these pioneering studies were concerned with dipolar "push-pull" structures arising from 4,5- and 9,10-substitutions, which are also common for 1,8- and 1,3-substitutions. Thus, the unique features of the pyrene K-region have not yet been investigated systematically.

Herein, we propose that the introduction of *N,N*-dialkylamino groups at the pyrene K-region, especially at the 4,5-position, activates aggregation-induced emission (AIE).[17,18] We have previously demonstrated[19] that highly twisted *N,N*-

Received: April 26, 2017
Published: June 28, 2017

DOI: 10.1021/acs.joc.7b00996
J. Org. Chem. 2017, 82, 6865−6873

dialkylamino groups at the appropriate positions efficiently stabilize the S_1/S_0 minimum energy conical intersection (MECI), through which electronic excitation energy is dissipated efficiently into vibrational energy.[20] In general, low-lying S_1/S_0 MECIs under concomitant large deformation are likely to occur in AIE. While low-lying MECIs enable a fast $S_0 \leftarrow S_1$ internal conversion in solution, large deformations are usually restricted by the molecular surrounding. In fact, *N,N*-dialkylaminoarenes we proposed have displayed faint fluorescence in solution, but bright fluorescence in restricted media such as the solid state.[19] The appropriate positions for the twisted *N,N*-dialkylamino groups are those positions, where donors facilitate the deformation toward a S_1/S_0 MECI structure. Taking linear acenes as an example, *para*-substitution of the *N,N*-dialkylamino groups stabilizes the bond between the bridgehead positions of the Dewar-benzene-like S_1/S_0 MECI.[19] When this design strategy is applied to pyrene, the unique features of the pyrene K-region become evident (Figure 1a).

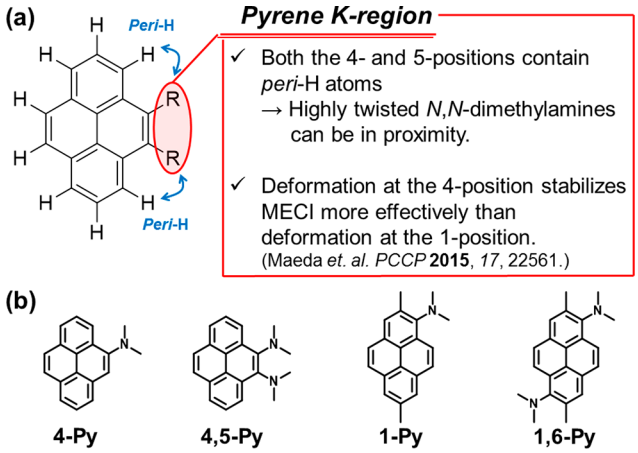

Figure 1. (a) Pyrene K-region and (b) the highly twisted mono- and bis(*N,N*-dimethylamino)pyrenes used in this study.

First, substituents at both the 4- and 5-positions are subject to severe steric repulsion from the *peri*-hydrogen atoms. Thus, both adjacent *N,N*-dimethylamino groups should be highly twisted, which may result in cooperative stabilization of the S_1/S_0 MECI. Second, theoretical investigations conducted by Maeda and co-workers revealed that deformations at the 4-position afford more stable S_1/S_0 MECIs for unsubstituted pyrenes than deformations at the 1-position.[21] This result implies that a strong donor at the 4-position may stabilize the S_1/S_0 MECI more effectively than at the 1-position.

Consequently, *N,N*-dialkylamino groups at the 4,5-positions are likely to activate AIE. The present study examines the photophysical properties of 4,5-bis(*N,N*-dimethylamino)pyrene (**4,5-Py**) in solution and the solid state. For comparison, the less twisted 4-(*N,N*-dimethylamino)pyrene (**4-Py**) and other regioisomers, i.e., **1-Py** and **1,6-Py**, which possess highly twisted *N,N*-dimethylamines at the 1- and 1,6-positions are also examined (Figure 1b).

RESULTS AND DISCUSSION

Synthesis and Characterization. As illustrated in Scheme 1, 4-(*N,N*-dimethylamino)pyrene (**4-Py**) and 4-(*N,N*-dimethylamino)pyrene (**4,5-Py**) were synthesized via a four-step reaction from pyrene. Initially, pyrene was converted into 4,5-diketopyrene (**2**) using a ruthenium-catalyzed oxidation.[22] Subsequently, 4,5-diaminopyrene (**4a**) was prepared following the method reported by Anzenbacher and co-workers.[23] Although **4a** was obtained as a crude mixture including 4-aminopyrene (**4b**) and other byproducts, this crude mixture underwent permethylation, because (i) **4a** is susceptible to oxidation and quickly decomposes into **2** during purification under ambient conditions, and (ii) permethylation of the crude mixture should afford **4-Py** and **4,5-Py** simultaneously. This notion is supported by previous reports,[19] which describe that the permethylation of sterically congested amines stops at the tertiary amine stage regardless of stoichiometry.

The aryl-N bonds of **1-Py** and **1,6-Py** are severely twisted due to the presence of methyl groups at the 2,7-positions. To introduce methyl groups at the 2,7-positions, pyrene 2,7-bis(boronic acid pinacol ester) (**5**) was brominated[24] and subsequently methylated using *n*-butyllithium and methyl iodide (Scheme 2). The thus obtained 2,7-dimethylpyrene (**7**) was sufficiently soluble in various organic solvents. Addition of nitric acid (2 equiv) at $T < 10$ °C resulted in a selective mononitration, while nitration at $T = 90$ °C afforded a mixture containing **8b** and various other byproducts. In general, the separation of regioisomers of pyrenes disubstituted at the 1-, 3-, 6-, 8-positions, is not easy,[1,10] and low solubility of the nitrated mixtures renders the purification even more difficult. Thus, the reduction and permethylation of the mixture containing **8b** were carried out before **1,6-Py** was isolated from the mixture. Other regioisomers could not be isolated in analyzable amounts. **4-Py**, **4,5-Py**, **1-Py**, and **1,6-Py** were fully characterized by ^{1}H NMR, ^{13}C NMR (Figure S1–S18), and FT-IR spectroscopy, high-resolution mass spectrometry

Scheme 1. Synthesis of 4-Py and 4,5-Py

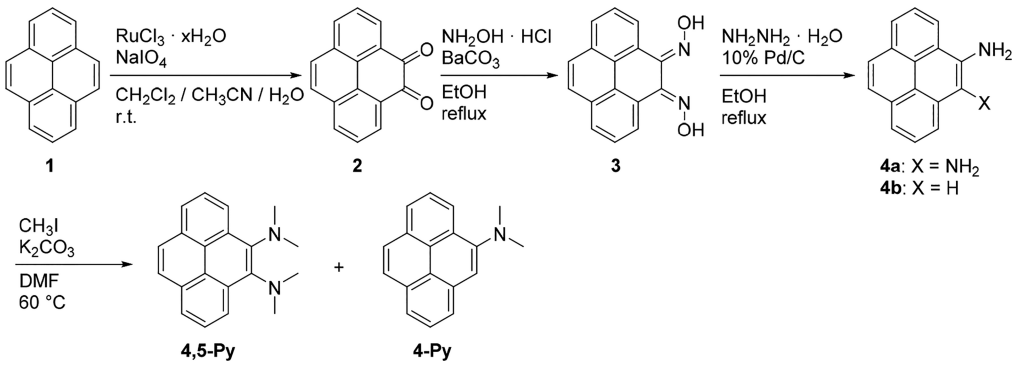

DOI: 10.1021/acs.joc.7b00996
J. Org. Chem. 2017, 82, 6865–6873

Scheme 2. Synthesis of 1-Py and 1,6-Py

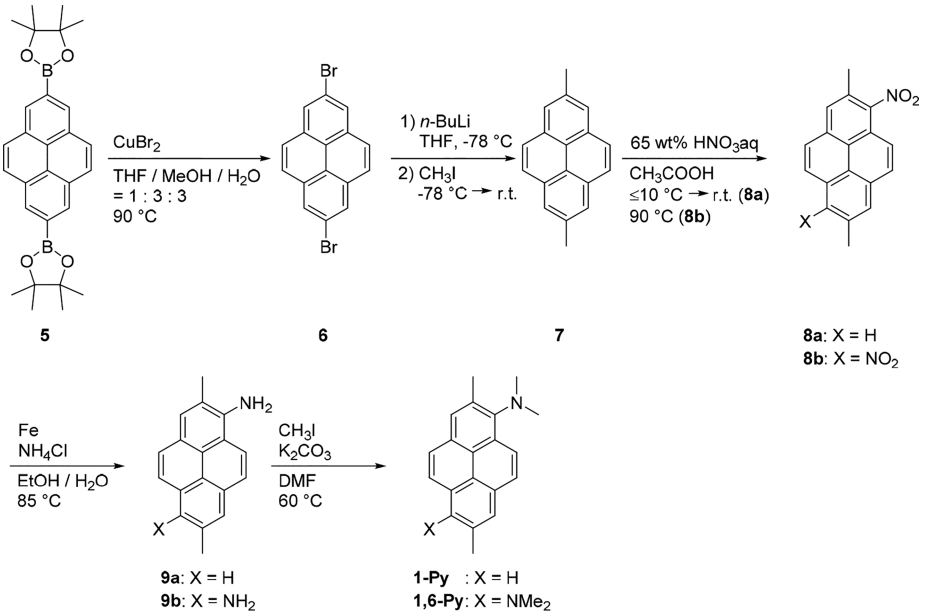

Table 1. Fluorescence Quantum Yields (Φ_{fl}), as well as Radiative (k_r) and Nonradiative Rate Constants (k_{nr}) of Acetonitrile Solutions, Colloidal Suspensions (THF/H_2O, 1/9, v/v), and Polycrystalline Solids of 4-Py, 4,5-Py, 1-Py, and 1,6-Py

	acetonitrile solution			colloidal suspension[a]			polycrystalline solids
entry	Φ_{fl}	k_f[b] [10^7 s^{-1}]	k_{nr}[b] [10^7 s^{-1}]	Φ_{fl}	k_f[b] [10^7 s^{-1}]	k_{nr}[b] [10^7 s^{-1}]	Φ_{fl}[c]
4-Py	0.93	7.87	0.57	0.67	3.69	1.82	0.46
4,5-Py	0.04	2.44	57.1	0.40	3.63	5.39	0.49
1-Py	0.24	5.71	18.3	0.40	2.21	3.35	0.63
1,6-Py	0.48	10.1	11.0	0.03	–	–	0.03

[a]Aggregation was confirmed by a broadening of the corresponding UV–vis spectra (Figure S23). [b]The amplitude-average lifetime was used for samples with multiexponential decays.[33] [c]Excitation wavelength: λ_{ex} = 350 nm.

(HRMS), and melting point analysis. The integrity of the K-region in **1-Py** and **1,6-Py** was confirmed by an analysis of the ^{1}H–^{1}H COSY NMR spectra (Figures S14 and S19).

The absorption spectra of **4-Py**, **4,5-Py**, **1-Py**, and **1,6-Py** feature two shoulders at ~390–380 nm and ~360–370 nm, in addition to the vibronic bands at ~340, ~330, and ~315 nm (Figure S20). While the structures of the vibronic bands are somewhat blurred due to the overlap with the $S_0 \rightarrow {}^1$CT transitions (probably at 300–400 nm), the vibronic structures are clearly observed in the absorption and fluorescence spectra in formic acid (Figure S22). Such vibronic structures are common in unsubstituted pyrenes in solution,[25,26] single crystals,[27] and various substituted pyrenes.[28−32] According to Platt's notation, small absorption bands at ~390–380 nm and ~360–370 nm should be assigned to the $S_0 \rightarrow {}^1L_b$ transition, which is almost entirely hidden in the $S_0 \rightarrow {}^1$CT transition band, while the structured band at ~340–315 nm should be assigned to the $S_0 \rightarrow {}^1L_a$ transition.[26] The strength of the $S_0 \rightarrow {}^1L_b$ band and the vibronic peaks of the $S_0 \rightarrow {}^1L_a$ band fluctuate largely in response to changing solvent polarity[32] and substitution pattern.[28,30]

Aggregation-Induced Emission of 4,5-Py. As shown in Table 1, **4,5-Py** features faint fluorescence in acetonitrile (Φ_{fl} = 0.04), but intense fluorescence in colloidal suspensions (Φ_{fl} = 0.40) and as a polycrystalline solid (Φ_{fl} = 0.49). Conversely, **4-Py**, **1-Py**, and **1,6-Py** exhibit moderate to high Φ_{fl} values in acetonitrile, which increase slightly or decrease in colloidal suspensions and polycrystalline solids, respectively. Among these pyrene derivatives, **4-Py** was the most fluorescent except in *n*-hexane (Table S1), where some pyrene-based dyes suffer from fast intersystem crossing (ISC).[29] The Φ_{fl} of **4,5-Py**, **1-Py**, and **1,6-Py** declines with increasing solvent polarity (Table S1), but **4,5-Py** is nevertheless far less fluorescent than **1-Py** and **1,6-Py**, both in polar and nonpolar solvents. These differences in Φ_{fl} arise mainly from the differences in the nonradiative transition rate constant, k_{nr}. The order of the k_{nr} values for this series in THF is **4-Py** (k_{nr} = 1.10 × 10^7 s^{-1}) < **1,6-Py** (3.83 × 10^7 s^{-1}) ≈ **1-Py** (4.57 × 10^7 s^{-1}) ≪ **4,5-Py** (13.1 × 10^7 s^{-1}), while that of the k_{nr} values in acetonitrile is **4-Py** (k_{nr} = 0.57 × 10^7 s^{-1}) ≪ **1,6-Py** (11.0 × 10^7 s^{-1}) < **1-Py** (18.3 × 10^7 s^{-1}) ≪ **4,5-Py** (57.1 × 10^7 s^{-1}). On the other hand, the radiative transition rate constant, k_r, accounts only for the weak fluorescence in **4,5-Py**, while the k_r values of **1-Py** and **1,6-Py** are larger than that of fluorescent **4-Py**. Therefore, it can be concluded that the presence of highly twisted *N*,*N*-dialkylamino groups, especially at the 4,5-position, induces fast nonradiative transitions both in polar and nonpolar solvents, resulting in faint fluorescence in solution.

Aggregation-induced emission (AIE) from **4,5-Py** was clearly demonstrated in THF/water mixtures (Figure 2). In the water fraction range f_w = 0–70 vol %, the fluorescence intensity declines with increasing solvent polarity of the solvent, which is enhanced by water, while the fluorescence intensity increases dramatically at f_w > 80 vol % (Figure 2b). This AIE of **4,5-Py** is

DOI: 10.1021/acs.joc.7b00996
J. Org. Chem. 2017, 82, 6865–6873

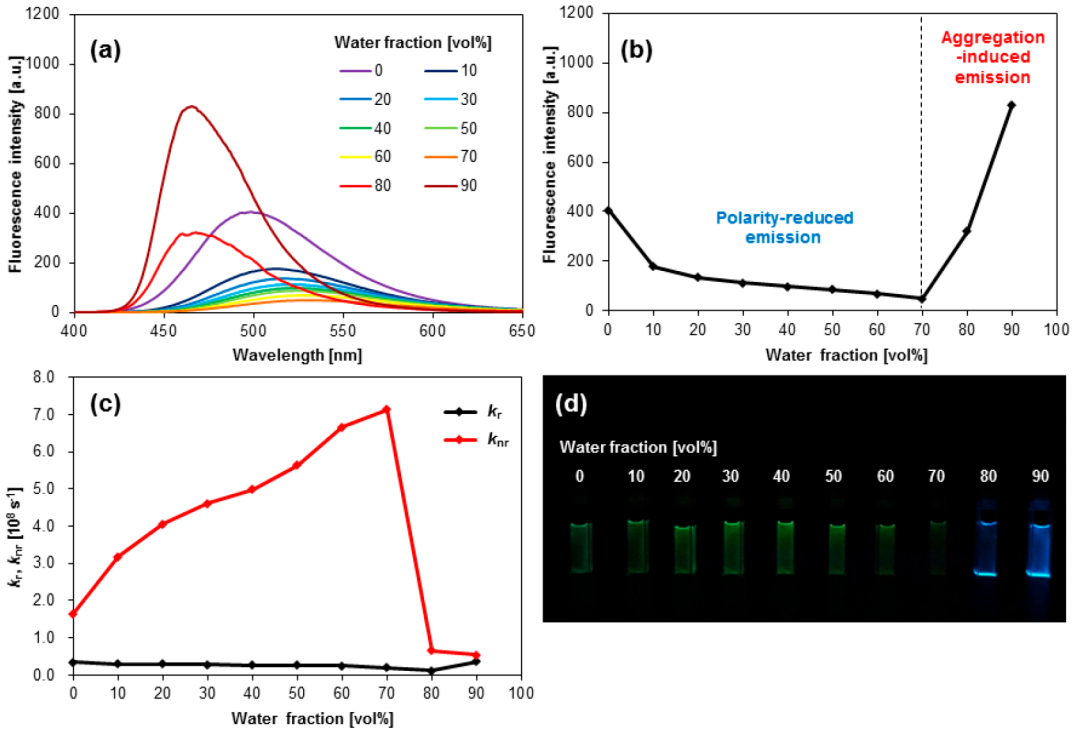

Figure 2. (a) Fluorescence spectra, (b) maximum fluorescence intensities, (c) radiative (k_r) and nonradiative (k_{nr}) transition rate constants, as well as (d) photographic images (λ_{irr} = 365 nm) of **1,4-Py** in THF/water mixtures with varying water content.

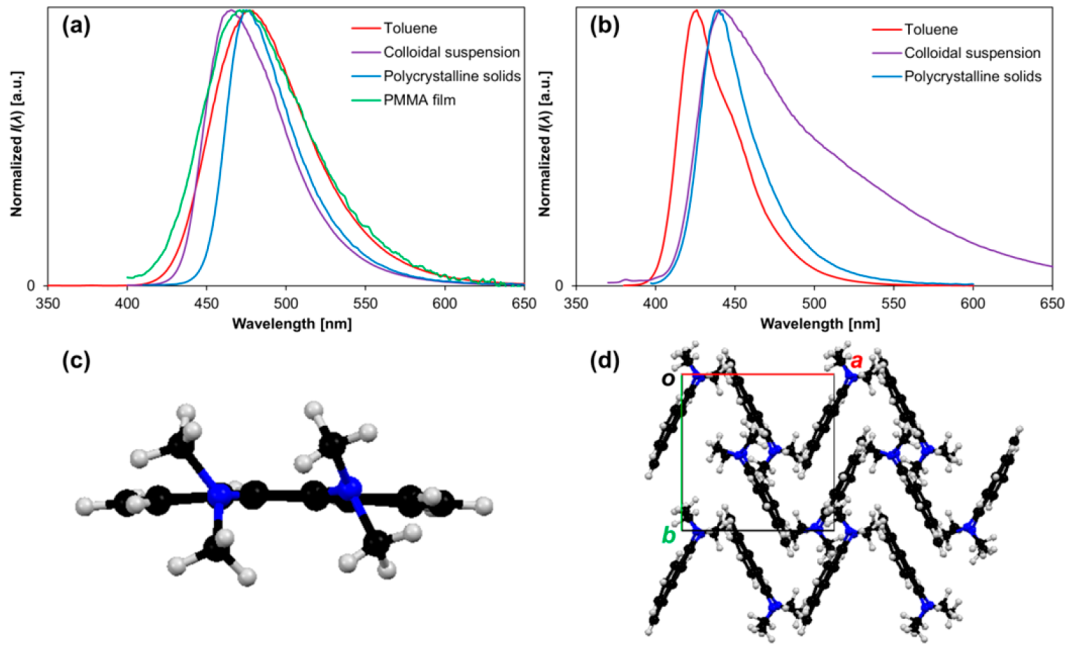

Figure 3. Fluorescence spectra of (a) **4,5-Py** and (b) **1-Py** measured in toluene solution, colloidal suspension (THF/H_2O, 1/9, v/v), and on polycrystalline solids. The fluorescence spectrum of **4,5-Py** dispersed in a PMMA film (**4,5-Py**/PMMA, 3.3/10 000, w/w) is also shown; (c), (d) Molecular structures of **4,5-Py** derived from X-ray crystallography.

due to the suppression of nonradiative transitions. In order to estimate radiative and nonradiative rate constants, the multi-exponential decays observed in the THF/water mixtures must be approximated to a single component. Amplitude-averaged lifetimes were adopted for these calculations, as they provide a good approximation for systems in which fluorescent molecules are exposed to different environments.[33,34] The thus obtained radiative and nonradiative rates (Figure 2c) demonstrate that both the polarity-reduced emission and the AIE of **4,5-Py** can be rationalized in terms of the large fluctuation of nonradiative rates, while the radiative rates remained almost constant over the entire f_w range. The polarity-reduced emission and AIE of **4,5-Py** are accompanied by a continuous bathochromic shift and a drastic hypsochromic shift, respectively (Figure 2). Similar behavior has previously been reported for D−π−A based AIEgens, whose hypsochromic shift upon aggregation

DOI: 10.1021/acs.joc.7b00996
J. Org. Chem. 2017, 82, 6865−6873

was attributed to restricted intramolecular motion and inefficient solvation in the solid states.[35] As demonstrated in previous studies,[10,36,37] nonradiative transitions of substituted pyrene derivatives, especially in polar solvents, are governed by the internal $S_0 \leftarrow S_1$ conversion rather than by ISCs.

Even though unsubstituted pyrene exhibits strong excimer fluorescence both in single crystals (Φ_{fl} = 0.68)[27,38] and in milled fine powders (Φ_{fl} = 0.67),[38] and although various substituted pyrenes feature broad and bathochromically shifted excimer fluorescence in crystals[39,40] and thin-films,[11,41,42] the AIE of **4,5-Py** should not arise from excimer formation or other excitonic interactions with neighboring chromophores, due to the following reasons: (i) both colloidal suspensions and polycrystalline solids of **4,5-Py** exhibit narrower fluorescence bands than the toluene solutions and dispersions in PMMA films (**4,5-Py**/PMMA, 3.3/10 000, w/w) at similar wavelengths (Figure 3a); (ii) the diffuse-reflectance spectrum of a 1 mM dispersion of **4,5-Py** in NaBr does not exhibit any sharp and intense peaks in the longer-wavelength region (Figure S25), which rules out a potential drastic increase of k_r upon the selective formation of *J*-aggregates;[43] (iii) the X-ray diffraction analysis of **4,5-Py** (Figure 3c,d) revealed the absence of close contacts and face-to-face packing. The observed distances between neighboring pyrene rings (along the *a*-axis: 7.80 Å, along the *b*-axis: 9.72 Å, and along the *c*-axis: 9.23 Å) are too long to allow the formation of excimers.[44] Taking it also into account that the k_r of **4,5-Py** is not enhanced significantly upon aggregation (Figure 2c), the aggregation of **4,5-Py** should be considered as a means to restrict intramolecular vibrations rather than as a means to generate other fluorescent species via electronic interactions with neighboring chromophores.

1-Py also exhibits higher Φ_{fl} in colloidal suspensions and polycrystalline solids than in acetonitrile solution (Φ_{fl} = 0.24), although the latter value is too high for **1-Py** to be regarded as an AIEgen (Table 1). The mechanism for the enhancement of Φ_{fl} in **1-Py** seems to be complicated. As shown in Figure 3b, the fluorescence spectra of **1-Py** greatly vary between the toluene solution, colloidal suspensions, and the polycrystalline solids. The broad emission band at ~500−600 nm appears only in the spectrum of the colloidal suspension of **1-Py**, which coincides with a long-lifetime component ($\tau \approx 30$ ns) at the fluorescence maximum (λ_{fl} = 442 nm). The long-lifetime component becomes more significant when the fluorescence decay is measured at 550 nm (Table S1). The long-lived excited species with broad and red-shifted fluorescence should thus be assigned to an excimer between neighboring chromophores.

Compared to the corresponding solutions, the Φ_{fl} values of **4-Py** decline in colloidal suspensions and polycrystalline solids, with contributions from both a decreased k_r and an increased k_{nr} (Table 1 and S1). Faint solid-state fluorescence was observed for **1,6-Py** (Table 1) and its fluorescence spectrum was substantially more red-shifted and broader than those of the solutions (Figure S23 and S26). In addition, the excitation of **1,6-Py** at ~450−500 nm led to the emergence of a broad fluorescence band at ~500 nm with enhanced Φ_{fl} (Figure S26 and S27). Self-absorption may be a possible reason for the fluorescence quenching in **1,6-Py**, as its diffuse-reflectance (Figure S25) largely overlaps with its fluorescence spectrum in solution (Figure S21). Efficient self-absorption renders an excited state more likely to be trapped in nonfluorescent defect sites. However, the underlying mechanisms for the fluorescence quenching in **4-Py** and **1,6-Py** in the solid state are beyond the scope of this study, given that such excitonic interactions in molecular crystals must be analyzed by stationary or transient-absorption spectra of large single crystals or on crystalline thin films. On the other hand, the ultimate objective of this study is to design AIE luminogens with unique internal conversions that are fast in solution but suppressed in the solid state.

The Violation of the Energy-Gap Law. As predicted by our design strategy, the introduction of strongly twisted *N*,*N*-dimethylamines at the pyrene K-region induced a drastic AIE in the resulting materials. The AIE is most likely due to a suppression of intramolecular vibrations, i.e., to internal conversions. Our design strategy is based on the assumption that AIE is activated by internal conversion through low-lying MECIs.[19] In order to confirm this hypothesis, the extremely fast nonradiative transition for **4,5-Py** will be discussed. According to Englman's formulation,[45] the rate constants for nonradiative transitions are mainly determined by the activation energy toward MECIs in cases where the structural difference between the ground and the excited states is large and where these two surfaces cross at energetically accessible points. This kind of cases has been defined as "strong coupling limit". On the other hand, $S_0 \leftarrow S_1$ internal conversion is still possible even for cases where the structural difference between the two states is small and when these two surfaces cross at energetically inaccessible points. In this "weak coupling" case, the $S_0 \leftarrow S_1$ internal conversion is accelerated by a narrow S_0-S_1 gap due to a larger Franck−Condon factor, i.e., vibrational overlap around the S_1 minimum geometry, which represents the well-known "energy-gap law".[45] To underscore the importance of tuning MECI, k_{nr} of **4,5-Py** should be rationalized in terms of energetics other than the energy-gap law.

4,5-Py exhibits the narrowest S_0-S_1 gap among all pyrene derivatives examined in this study. With increasing solvent polarity parameter $E_T(30)$,[46] the fluorescence maxima of these pyrene derivatives are bathochromically shifted in a linear fashion (Figure 4), which indicates that their fluorescence

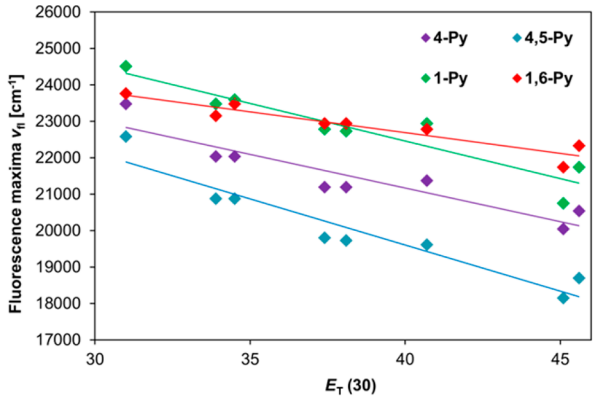

Figure 4. Fluorescence maxima of **4-Py**, **4,5-Py**, **1-Py**, and **1,6-Py** as a function of the solvent polarity parameter E_T (30).[46]

should be attributed to $S_0 \leftarrow {}^1CT$ transitions. Regardless of the solvent polarity, the fluorescence of **4,5-Py** is of lower energy than that of **4-Py**, **1-Py**, and **1,6-Py**, reflecting the narrow S_0-S_1 gap of **4,5-Py**. In addition to intramolecular effects, strong solvent−solute interactions are responsible for the narrow S_0-S_1 gap, due to the dipolar structure of **4,5-Py**. The incremental changes of the dipole moments upon photoexcitation (**4-Py**: 6.0 D; **4,5-Py**: 7.0 D; **1-Py**: 6.1 D; **1,6-Py**: 4.0 D) were estimated using a Lippert−Mataga plot (Figure S24).[47] Strong solvent−solute interactions for **4,5-Py** are also reflected in its

DOI: 10.1021/acs.joc.7b00996
J. Org. Chem. 2017, 82, 6865−6873

full width at half maxima (fwhm), which is given by the reduced intensity[48] [$L(\nu) = I(\nu)/\nu^3 = I(\lambda)/\nu^5$] in acetonitrile (**4,5-Py**: 4200 cm^{-1}; **1-Py**: 3900 cm^{-1}; **4-Py**: 3600 cm^{-1}; **1,6-Py**: 3200 cm^{-1}).

However, in order for this series to obey the energy-gap law, **4-Py** has to show a faster nonradiative decay than **1-Py** and **1,6-Py**. Thus, it can be anticipated that these molecules should rather correspond to the "strong coupling" case. This hypothesis is further supported by a comparison of the k_{nr} values of other pyrene derivatives. For example, some alkylaminopyrenes have far smaller k_{nr} values (~$0.5-1.5 \times 10^7$ s^{-1})[10,36] than **4,5-Py** (57.1×10^7 s^{-1}), while their fluorescence maxima are located around 17 000–20 000 cm^{-1}, which is virtually identical to the value (18 700 cm^{-1}) for **4,5-Py** in acetonitrile. Therefore, it can be concluded that **4,5-Py** exhibits a substantially faster internal conversion than the other alkylaminopyrene derivatives. Since the MECIs of typical rigid aromatic hydrocarbons are too high to be accessed thermally, they are subject to slow $S_0 \leftarrow S_1$ internal conversions, which is consistent with the energy-gap law[49] and leads to strong fluorescence in solution. In contrast, **4,5-Py** should undergo fast $S_0 \leftarrow S_1$ internal conversion via MECI, which should result in AIE. Thus, *N,N*-dialkylamino groups at the 4,5-positions of pyrene should promote fast internal conversion via MECI as well as rotational vibrations around isomerizable double bonds[50] or multiple aryl–aryl bonds[51] in various AIEgens.[18]

CONCLUSION

In summary, pyrene can successfully be endowed with AIE functionality simply by introducing two strongly twisted *N,N*-dimethylamines at the pyrene K-region. Conversely, the introduction of strongly twisted *N,N*-dimethylamines at the 1- and 1,6-positions resulted in intense fluorescence in solution. These differences are attributed mainly to nonradiative transitions. A comparison of the k_{nr} value of **4,5-Py** with its fluorescence energetics implies the involvement of a special pathway, e.g., a nonadiabatic relaxation via MECI, for efficient internal conversions. These results demonstrate the viability of our AIEgen design strategy based on the concept of MECIs, which should also be applicable to nonlinear acenes. Moreover, to the best of our knowledge, this is the first study that capitalizes on the unique features of the pyrene K-region, i.e., the steric repulsion that arises from the presence of two *peri*-hydrogens, to derive fluorescence functionality. Although synthetic methods to introduce different functional groups at the 4,5-positions have not yet been developed, such an asymmetric functionalization should allow the advanced molecular engineering of MECI in pyrenes. Thus, this study also demonstrates the importance of advancing the boundaries of synthetically controlling the regioselectivity of the pyrene K-region. A joint theoretical and experimental project to elucidate how neighboring *N,N*-dimethylamino groups stabilize MECIs effectively, and to establish general design strategies toward AIEgens based on ubiquitous aromatic hydrocarbons is currently in progress.

EXPERIMENTAL SECTION

General Procedures. ^1H and ^{13}C NMR spectra were recorded on a 300 MHz BRUKER DPX300 or 500 MHz BRUKER avance III spectrometer using tetramethylsilane (TMS) as the internal standard. FT-IR spectra were recorded on a JASCO FT-IR 469 plus spectrometer. Melting points were recorded on a Yanaco micro melting point MP-500P apparatus. Mass spectra (FAB and EI) were obtained using a JEOL JMS700 mass spectrometer, which uses a double-focusing reversed-geometry magnetic sector ("BE" type) as the mass analyzer.

UV–vis spectra were recorded on a JASCO V-670 UV–vis spectrophotometer. Fluorescence spectra were recorded on a JASCO FP-6500 spectrofluorometer. The wavelengths obtained with the fluorescence spectrometer were converted into wavenumbers using the equation $I(\tilde{\nu}) = \lambda^2 I(\lambda)$.[52] Absolute quantum yields (Φ_{fl}) were measured with a Hamamatsu Photonics Quantaurus QY apparatus. Fluorescence lifetime values at 298 K were obtained from the most intense peaks using a Hamamatsu Photonics OB 920 fluorescence lifetime spectrometer equipped with a LED lamp (λ_{ex} = 343 nm). Unless otherwise noted, all photophysical measurements in solution were carried out at 298 K using dilute solutions with optical densities (ODs) of ~0.1 at the maximum absorption wavelength in quartz cells (path length: 1 cm). In addition, all sample solutions were deaerated by argon sparging for 15 min prior to quantum yield and lifetime measurements. For measurements of the aggregates, colloidal suspensions (THF/H_2O, 1/9, v/v) with a concentration of 1.0×10^{-4} M were prepared, and aggregation was confirmed by the severe broadening of the UV–vis spectra (Figure S23).

Photophysical Measurements of Solid Samples. Prior to any photophysical measurements in the solid state, i.e., of polycrystalline solids, the measurements of dispersions in NaBr and colloidal suspensions (THF/H_2O, 1/9, v/v), recrystallization and subsequent fluorescence quantum yield measurements were repeated three times.[19,53] Polycrystalline solids were consecutively recrystallized from (i) methanol or dichloromethane/methanol mixtures, (ii) methanol or ethanol, and (iii) methanol at −10 °C. In the regions where **4-Py**, **4,5-Py**, and **1-Py** exhibit significant absorbance, fluorescence quantum yields were virtually independent from the excitation wavelength. For **1,6-Py**, excitation at ~450 nm induced a significantly higher fluorescence quantum yield compared to other excitation wavelengths (Figure S27). Repeated recrystallization, column chromatography, and high-performance liquid chromatography slightly enhanced the fluorescence quantum yields at ~450 nm, instead of removing it.

Diffuse-Reflectance Spectra. Diffuse-reflectance spectra were recorded on a JASCO FP-6500 spectrofluorometer equipped with an integration sphere detector. Thus, the experimental error arising from the fluorescence, which is typically encountered with diffuse-reflectance spectrometers producing polychromatic outgoing light, was avoided. Analyte and reference samples were charged in a JASCO powder sample cell in order to obtain a sufficiently thick powder layer. Immediately prior to each measurement, the synchronous reflectance spectrum of NaBr powder was measured in order to afford a standard reference, $r_{standard}(\lambda)$. Then, the reflectance spectrum of each sample, $r_{sample}(\lambda)$, was obtained following the same procedure. In addition to polycrystalline samples, the spectra of samples dispersed in NaBr powder were measured at a concentration of 1.0×10^{-3} M. The obtained reflectance spectra $r_{sample}(\lambda)$ and $r_{standard}(\lambda)$ were converted to Kubelka–Munk functions $f(r_\infty)$ using the following equation:[54]

$$f(r_\infty) = \frac{(1 - r_\infty(\lambda))^2}{2r_\infty(\lambda)}$$

where

$$r_\infty = \frac{r_{sample}(\lambda)}{r_{standard}(\lambda)}$$

All diffuse-reflectance spectra are displayed as plots of the Kubelka–Munk functions, i.e., the $f(r_\infty)$ is displayed as a function of the wavelength, λ.

Synthesis of 4,5-Diketopyrene (2).[22] A solution of pyrene (**1**; 2.0 g, 10 mmol) and ruthenium(III) chloride hydrate (0.2 g, 0.96 mmol) in dichloromethane (40 mL), acetonitrile (40 mL), and water (25 mL) was treated at 0 °C with sodium periodate (10 g, 47 mmol). The reaction temperature was kept at 0 °C for 10 min, before the reaction mixture was warmed to room temperature, where stirring was

DOI: 10.1021/acs.joc.7b00996
J. Org. Chem. 2017, 82, 6865–6873

continued for 15 h. The reaction mixture was poured onto water (800 mL) and extracted with dichloromethane (3 × 50 mL). The combined organic layers were washed with water (3 × 200 mL), brine, and dried over magnesium sulfate. After filtration, the solvent was removed in vacuo, and the thus obtained residue was purified by column chromatography on silica gel (eluent: CH_2Cl_2) to yield crude 4,5-diketopyrene (**2**; 0.91 g) as a bright orange solid. Yield: 39%; ^{1}H NMR (300 MHz, $CDCl_3$) δ 8.47 (d, ^4J = 1.2 Hz, ^3J = 7.5 Hz, 2H), 8.16 (d, ^4J = 1.2 Hz, ^3J = 7.9 Hz, 2H), 7.83 (s, 2H), 7.74 (t, ^3J = 7.8 Hz, 2H) ppm.

Synthesis of 4,5-Diketopyrene dioxime (3).[23] Prior to the reaction, the reaction apparatus was flame-dried in vacuo. Under an atmosphere of argon, a solution of **2** (0.88 g, 3.8 mmol), hydroxylamine hydrochloride (0.93 g, 13 mmol), and barium carbonate (1.1 g, 5.7 mmol) in dehydrated ethanol (50 mL) was kept at reflux for 120 h. During this time, the initial orange slurry gradually turned colorless. After the reaction mixture had been cooled to 60 °C, the solvent was removed in vacuo. Then, a 0.2 M aqueous solution of hydrochloric acid (60 mL) was added, and the resulting suspension was stirred at room temperature for 30 min. Subsequently, the suspension was filtered and the residue was washed with water, ethanol, and diethyl ether. The thus obtained residue was dried in vacuo to afford crude 4,5-diketopyrene dioxime (**3**; 1.0 g) as a pale yellow solid, which was used in the subsequent reaction step without further purification. Yield: ≥ 99%; ^{1}H NMR (300 MHz, DMSO-d_6) δ 13.43 (s, 1H), 12.96 (s, 1H), 9.06 (d, ^3J = 7.3 Hz, 1H), 8.24 (d, ^3J = 7.7 Hz, 1H), 8.15 (d, ^3J = 7.8 Hz, 1H), 8.09 (d, ^3J = 7.8 Hz, 1H), 7.95 (s, 2H), 7.80 (t, ^3J = 7.9 Hz, 1H), 7.73 (t, ^3J = 7.4 Hz, 1H) ppm.

Synthesis of 4,5-Diaminopyrene (4).[23] Hydrazine monohydrate (7.5 mL, 154 mmol) was added dropwise over 1 h to a stirred solution of **3** (1.0 g, 3.8 mmol) and Pd on carbon (Pd: 10%) wetted with 55% water (1.3 g, 0.56 mmol) in ethanol (32 mL), which was kept at reflux. The reaction mixture was kept at reflux for another 48 h, before the hot reaction mixture was filtered and washed with boiling ethanol. Immediately thereafter, all volatiles were removed in vacuo, and cold water was added, before the mixture was stored at 0 °C for 12 h. Subsequently, the thus obtained slurry was filtered, and the isolated solid was washed with cold water. The residue was dried in vacuo to afford crude 4,5-diaminopyrene (**4**), which contained a considerable amount of impurities. Despite the low purity, the crude product was, given its sensitivity to air, used in the next reaction step without further purification. ^{1}H NMR (300 MHz, DMSO-d_6) δ 8.33 (dd, ^4J = 1.4 Hz, ^3J = 7.6 Hz, 2H), 8.07 (s, 2H), 8.01 (dd, ^4J = 1.4 Hz, ^3J = 7.5 Hz, 2H), 7.96 (t, ^3J = 7.5 Hz, 2H), 5.22 (s, 4H) ppm.

Synthesis of 4,5-Bis(*N*,*N*-dimethylamino)pyrene (4,5-Py). A stirred solution of crude **4** (≤0.89 g, ≤ 3.8 mmol) and potassium carbonate (3.2 g, 23 mmol) in dehydrated DMF (40 mL) was treated with methyl iodide (1.9 mL, 31 mmol) and the reaction mixture was stirred at 60 °C for 12 h. Then, the reaction mixture was extracted with ethyl acetate/hexane (1/4; v/v). The combined organic layers were washed with water and brine, before being dried over magnesium sulfate. After filtration, the solvent was removed in vacuo, and the thus obtained residue was purified by column chromatography on silica gel (eluent: hexane/ethyl acetate, 10/1, v/v). The crude product was further purified by high-performance liquid chromatography to yield crude **4,5-Py** (0.13 g) as a colorless solid. Another fraction obtained from high-performance liquid chromatography contained 4-(*N*,*N*-dimethylamino)pyrene (**4-Py**) (0.12 g) as a colorless solid. **4,5-Py** was recrystallized several times from methanol in order to enhance its purity. Yield: 12%; mp 169.8−170.8 °C; ^{1}H NMR (300 MHz, $CDCl_3$) δ 8.43 (dd, ^4J = 1.1 Hz, ^3J = 7.9 Hz, 2H), 8.10 (dd, ^4J = 1.1 Hz, ^3J = 7.6 Hz, 2H), 8.02 (s, 2H), 7.98 (t, ^3J = 7.8 Hz, 2H), 3.17 (s, 12H) ppm; ^{13}C NMR (75 Hz, $CDCl_3$) δ 144.8, 132.1, 131.3, 127.1, 125.6, 124.4, 124.2, 122.1, 44.4 ppm; FT-IR (KBr) 1582 (Ar ring stretch), 1491 (Ar ring stretch), 1320 (Ar−N stretch), 835, 723 (Ar−H) cm^{-1}; HRMS (FAB/BE) m/z [M]$^+$ Calcd for $C_{20}H_{20}N_2$ 288.1626, found 288.1627.

4-Py: This compound was obtained as a byproduct from the synthesis of **4,5-Py**. The product was recrystallized several times from methanol in order to enhance its purity. Yield: 13%; mp 93.8−94.1 °C; ^{1}H NMR (300 MHz, $CDCl_3$) δ 8.55 (dd, ^4J = 1.0 Hz, ^3J = 7.9 Hz, 1H), 8.15 (dd, ^4J = 1.0 Hz, ^3J = 7.6 Hz, 1H), 8.06 (dd, ^4J = 1.0 Hz, ^3J = 7.6 Hz, 1H), 8.05−8.02 (m, 2H), 8.01 (t, ^3J = 7.9 Hz, 1H), 8.00 (d, ^3J = 9.0 Hz, 1H) 7.92 (t, ^3J = 7.6 Hz, 1H), 7.59 (s, 1H), 3.07 (s, 6H) ppm; ^{13}C NMR (75 Hz, $CDCl_3$) δ 149.8, 131.8, 131.6, 130.9, 128.2, 127.3, 127.1, 126.0, 125.9, 125.3, 125.1, 124.0, 123.4, 122.1, 121.8, 113.4, 45.0 ppm; FT-IR (KBr) 1592 (Ar ring stretch), 1491 (Ar ring stretch), 1315 (Ar−N stretch), 832, 732 (Ar−H) cm^{-1}; HRMS (FAB/BE) m/z [M]$^+$ Calcd for $C_{18}H_{15}N$ 245.1204, found m/z = 245.1204.

Synthesis of 2,7-Dibromopyrene (6).[24] A stirred solution of **5** (0.45 g, 0.99 mmol) in THF (10 mL) and methanol (30 mL) was treated with a solution of copper(II) bromide (4.3 g, 19 mmol) in water (30 mL) at room temperature. The reaction mixture was stirred at 90 °C for 12 h, before being concentrated under reduced pressure. Water (100 mL) was added to the thus obtained residue and the resulting white precipitate was collected by filtration and consecutively washed with water, diethyl ether, and hexane. The thus obtained white solid was extracted into hot toluene and filtered, before the solvent was removed in vacuo to yield a mixture of **5** and **6** (**5**:**6** = 41:59). Compound **5** was extracted from the mixture into boiling acetone, while the remaining insoluble white solid consisted of 2,7-dibromopyrene (**6**; 0.35 g). Yield: 98%; ^{1}H NMR (300 MHz, $CDCl_3$) δ 8.31 (s, 4H), 8.01 (s, 4H) ppm.

Synthesis of 2,7-Dimethylpyrene (7). The entire reaction apparatus was flame-dried in vacuo prior to any reaction. A 2.6 M solution of *n*-butyllithium in hexane (0.77 mL, 2.0 mmol) was added dropwise to a solution of **6** (0.33 g, 0.91 mmol) in anhydrous THF (100 mL) at −50 °C under an atmosphere of argon. The reaction mixture was stirred for 5 h at −25 °C, before methyl iodide (0.18 mL, 3.0 mmol) was added dropwise at −50 °C. The resulting mixture was gradually warmed to room temperature over the course of 12 h. The reaction was quenched by addition of water, before the reaction mixture was extracted with chloroform, and washed with water and brine. The combined organic layers were dried over magnesium sulfate and filtered. The solvent was removed from the filtrate in vacuo, and the obtained residue was purified by column chromatography on silica gel (eluent: chloroform). The crude product was further purified by recrystallization from dichloromethane/ethanol (1/5, v/v) to furnish crude 2,7-methylpyrene (**7**; 0.15 g) as a colorless solid, which was used in the next reaction step without further purification. Yield: 73%; ^{1}H NMR (300 MHz, $CDCl_3$) δ 7.97 (s, 4H), 7.96 (s, 4H), 2.78 (s, 6H) ppm; HRMS (FAB/BE) m/z [M]$^+$ Calcd for $C_{18}H_{14}$ 230.1096, found 230.1099.

Synthesis of 1-Nitro-2,7-dimethylpyrene (8a). An aqueous solution of nitric acid (65 wt %, 0.067 mL, 0.96 mmol) was added in one portion to a solution of **7** (0.11 g, 0.48 mmol) in glacial acetic acid (5 mL) maintained in an ice-bath in order to keep the temperature below 10 °C. Subsequently, the mixture was stirred at room temperature for 8 h, before being poured onto an aqueous solution of potassium carbonate (1.4 M, 100 mL). The thus obtained precipitate was extracted with chloroform, and the combined organic phases were washed with water and brine, before being dried over magnesium sulfate. After filtration, all volatiles were removed in vacuo, and the residue was purified by column chromatography on silica gel (eluent: chloroform) to afford crude 1-nitro-2,7-dimethylpyrene (**8a**) as a yellow solid (0.13 g, 0.47 mmol), which was used in the next reaction step without further purification. Yield: 98%; ^{1}H NMR (300 MHz, $CDCl_3$) δ 8.07 (d, ^3J = 9.3 Hz, 1H), 8.01 (d, ^3J = 9.3 Hz, 1H), 8.01 (m, 2H), 7.92 (s, 1H), 7.90 (d, ^3J = 9.3 Hz, 1H), 7.89 (d, ^3J = 9.3 Hz, 1H), 2.78 (s, 3H), 2.73 (s, 3H) ppm.

Synthesis of 1-Amino-2,7-dimethylpyrene (9a). A mixture of **8a** (0.13 g, 0.47 mmol), iron powder (0.093 g, 1.7 mmol), and ammonium chloride (0.063 g, 1.2 mmol) in aqueous ethanol (EtOH: 18 mL, H_2O: 5 mL) was kept at reflux for 12 h. The reaction mixture was filtered and the filtrate was extracted with ethyl acetate. The combined organic phases were consecutively washed with a saturated aqueous solution of potassium carbonate, water, and brine, before being dried over magnesium sulfate. After filtration, all volatiles were removed in vacuo to afford crude 1-amino-2,7-dimethylpyrene (**9a**; 0.12 g) as a brown solid, which was used in the next reaction step without further purification. Yield: 99%; ^{1}H NMR (300 MHz, $CDCl_3$)

DOI: 10.1021/acs.joc.7b00996
J. Org. Chem. 2017, 82, 6865−6873

δ 7.87 (s, 2H), 7.84−7.80 (m, 4H), 7.71 (d, ^3J = 8.9 Hz, 1H), 4.40 (brs, 2H), 2.72 (s, 3H), 2.54 (s, 3H) ppm.

Synthesis of 1-(*N*,*N*-Dimethylamino)-2,7-dimethylpyrene (1-Py). A mixture of crude **9a** (0.12 g, 0.47 mmol) and potassium carbonate (0.20 g, 1.4 mmol) in DMF (10 mL), was treated dropwise with methyl iodide (0.12 mL, 1.9 mmol), before the reaction mixture was stirred at 60 °C for 12 h. Further methyl iodide (0.12 mL, 1.9 mmol) was added, and stirring was continued at 60 °C for 4 h, before the reaction mixture was cooled to room temperature. The reaction mixture was extracted with ethyl acetate/hexane (1/4; v/v) and the combined organic fractions were washed with water and brine. Subsequently, the organic layer was dried over magnesium sulfate and the solvent was removed in vacuo after filtration. The thus obtained residue was purified by column chromatography on silica gel (eluent: hexane/ethyl acetate, 10/1, v/v). The crude product was further purified by recrystallization from methanol to afford 1-(*N*,*N*-dimethylamino)-2,7-dimethylpyrene (**1-Py**; 0.12 g) as a colorless solid. Yield: 94%; mp 144.8−145.9 °C; ^{1}H NMR (500 MHz, $CDCl_3$) δ 8.39 (d, ^3J = 9.2 Hz, 1H), 7.96 (d, ^3J = 9.2 Hz, 1H), 7.92 (s, 2H), 7.90 (d, ^3J = 8.9 Hz, 1H), 7.90 (s, 1H), 7.87 (d, ^3J = 8.9 Hz, 1H), 3.13 (s, 6H), 2.76 (s, 3H), 2.71 (s, 3H) ppm; ^{13}C NMR (75 MHz, $CDCl_3$) δ 145.9, 135.1, 134.7, 131.0, 130.9, 129.0, 128.4, 127.8, 126.8, 126.4, 126.2, 125.2, 125.1, 124.5, 124.3, 123.3, 43.8, 22.0, 19.9 ppm; FT-IR (KBr) 1588 (Ar ring stretch), 1489 (Ar ring stretch), 878, 858, 738 (Ar−H) cm^{-1}; HRMS (EI/BE) *m*/*z* [M]$^+$ Calcd for $C_{20}H_{19}N$ 273.1517, found 273.1521.

Synthesis of 1,6-Dinitro-2,7-dimethylpyrene (8b). An aqueous solution of nitric acid (65 wt %, 0.60 mL, 8.7 mmol) was added in one portion to a solution of **7** (0.5 g, 2.2 mmol) in glacial acetic acid (5 mL), which was maintained in an ice-bath in order to keep the temperature below 10 °C. The mixture was then stirred at 90 °C for 2 h, before being poured onto an aqueous solution of potassium carbonate (100 mL, 1.4 M). The thus obtained precipitate was extracted with chloroform and washed with water and brine. The combined organic layers were dried over magnesium sulfate, filtered, and all volatiles were removed in vacuo. The residue was purified by column chromatography on silica gel (eluent: toluene/chloroform, 4/1, v/v), which afforded three fractions. Removal of all volatiles from the first fraction furnished crude 1,6-dinitro-2,7-dimethylpyrene (**8b**) as a yellow solid (0.51 g, 1.6 mmol). The thus obtained crude product contained many impurities, but was nevertheless used in the next reaction step without further purification. Yield: 74%; ^{1}H NMR (300 MHz, $CDCl_3$) δ 8.10 (s, 2H), 8.08 (d, ^3J = 8.4 Hz, 2H), 8.03 (d, ^3J = 8.4 Hz, 2H), 2.78 (s, 6H) ppm.

Synthesis of 1,6-Diamino-2,7-dimethylpyrene (9b). A mixture of **8b** (0.51 g, 1.6 mmol), iron powder (0.63 g, 11 mmol), and ammonium chloride (0.43 g, 8.0 mmol) in aqueous ethanol (EtOH: 30 mL, H_2O: 8 mL) was kept at reflux for 12 h. The reaction mixture was filtered and the filtrate was extracted with ethyl acetate. The combined organic fractions were consecutively washed with a saturated aqueous solution of potassium carbonate, water, and brine. Then, the organic phase was dried over magnesium sulfate, before all volatiles were removed in vacuo to afford crude 1,6-diamino-2,7-dimethylpyrene (**9b**; 0.38 g) as a brown solid. Even though the thus obtained product contained many impurities, it was used for the next reaction step without further purification. Yield: 91%; ^{1}H NMR (300 MHz, $CDCl_3$) δ 7.80 (d, ^3J = 8.4 Hz, 2H), 7.78 (s, 2H), 7.68 (d, ^3J = 8.4 Hz, 2H), 4.35 (brs, 4H), 2.55 (s, 6H) ppm.

Synthesis of 1,6-Bis(*N*,*N*-dimethylamino)-2,7-dimethylpyrene (1,6-Py). A mixture of crude **9b** (0.38 g, 1.46 mmol) and potassium carbonate (1.0 g, 7.3 mmol) in DMF (25 mL) was treated dropwise with methyl iodide (0.63 mL, 10 mmol) and stirred at 60 °C for 12 h. More methyl iodide (0.63 mL, 10 mmol) was added and stirring was continued at 60 °C for 24 h, before the reaction mixture was cooled to room temperature. The reaction mixture was extracted with ethyl acetate/hexane (1/4; v/v) and washed with water and brine. Then, the combined organic layers were dried over magnesium sulfate, filtered, and all volatiles were removed in vacuo. The residue was purified by column chromatography on silica gel (eluent: hexane/ethyl acetate, 10/1, v/v). The crude product was further purified by high-performance liquid chromatography (eluent: chloroform) and recrystallization from dichloromethane/methanol (1/1; v/v) to afford 1,6-bis(*N*,*N*-dimethylamino)-2,7-dimethylpyrene (**1,6-Py**; 26 mg) as a pale yellow solid. Yield: 6%; mp 235.1−236.5 °C; ^{1}H NMR (300 MHz, $CDCl_3$) δ 8.31 (d, ^3J = 9.2 Hz, 2H), 7.90 (d, ^3J = 9.2 Hz, 2H), 7.90 (s, 2H), 3.12 (s, 12H), 2.71 (s, 6H) ppm; ^{13}C NMR (75 MHz, $CDCl_3$) δ 145.5, 134.8, 129.2, 128.4, 127.3, 126.1, 124.9, 123.4, 43.8, 19.9 ppm; FT-IR (KBr) 1589 (Ar ring stretch), 1482 (Ar ring stretch), 944, 870, 750 (Ar−H) cm^{-1}; HRMS (FAB/BE) *m*/*z* [M]$^+$ Calcd for $C_{22}H_{24}N_2$ 316.1939, found 316.1941.

■ ASSOCIATED CONTENT

Supporting Information

The Supporting Information is available free of charge on the ACS Publications website at DOI: 10.1021/acs.joc.7b00996.

Results of the ^{1}H and/or ^{13}C NMR spectra, data of absorption and fluorescence spectra, crystallographic information (PDF)

Crystal data (CIF)

■ AUTHOR INFORMATION

Corresponding Authors

*E-mail: shun.sasaki213@gmail.com.

*E-mail: konishi.g.aa@m.titech.ac.jp.

ORCID

Gen-ichi Konishi: 0000-0002-6322-0364

Notes

The authors declare no competing financial interest.

■ ACKNOWLEDGMENTS

This work was partially supported by a Grant-in-Aid for Scientific Research (Kakenhi) from the MEXT, Japan and S-Innovation from Japan Science and Technology Agency (JST).

■ REFERENCES

(1) Figueira-Duarte, T. M.; Mullen, K. *Chem. Rev.* **2011**, *111*, 7260−7314.

(2) (a) Feng, X.; Hu, J.-Y.; Redshaw, C.; Yamato, T. *Chem. - Eur. J.* **2016**, *22*, 11898−11916. (b) Ji, L.; Lorbach, A.; Edkins, R. M.; Marder, T. B. *J. Org. Chem.* **2015**, *80*, 5658−5665.

(3) (a) Eddaoudi, M.; Kim, J.; Rosi, N.; Vodak, D.; Wachter, M.; O'Keeffe, M.; Yaghi, O. M. *Science* **2002**, *295*, 469−472. (b) Rowsell, J. L. C.; Yaghi, O. M. *J. Am. Chem. Soc.* **2006**, *128*, 1304−1315. (c) Wong-Foy, A. G.; Matzger, A. J.; Yaghi, O. M. *J. Am. Chem. Soc.* **2006**, *128*, 3494−3495. (d) Ronson, T. K.; League, A. B.; Gagliardi, L.; Cramer, C. J.; Nitschke, J. R. *J. Am. Chem. Soc.* **2014**, *136*, 15615−15624.

(4) (a) Yagi, A.; Venkataramana, G.; Segawa, Y.; Itami, K. *Chem. Commun.* **2014**, *50*, 957−959. (b) Iwamoto, T.; Kayahara, E.; Yasuda, N.; Suzuki, T.; Yamago, S. *Angew. Chem., Int. Ed.* **2014**, *53*, 6430−6434.

(5) (a) Bernhardt, S.; Kastler, M.; Enkelmann, V.; Baumgarten, M.; Mullen, K. *Chem. - Eur. J.* **2006**, *12*, 6117−6128. (b) Gingras, M.; Placide, V.; Raimundo, J. M.; Bergamimi, G.; Ceroni, P.; Balzani, V. *Chem. - Eur. J.* **2008**, *14*, 10357−10363. (c) Figueira-Duarte, T. M.; Siman, S. C.; Wagner, M.; Drtezhinin, S. I.; Zachariasse, K. A.; Mullen, K. *Angew. Chem., Int. Ed.* **2008**, *47*, 10175−10178.

(6) (a) Percec, V.; Aqad, E.; Peterca, M.; Imam, M. R.; Gloddem, M.; Bera, T. K.; Miura, Y.; Balagurusamy, V. S. K.; Ewbank, P. C.; Wurthner, F.; Heiney, P. A. *Chem. - Eur. J.* **2007**, *13*, 3330−3345. (b) Sagara, Y.; Kato, T. *Nat. Chem.* **2009**, *1*, 605−610.

(7) (a) Niko, Y.; Didier, P.; Mely, I.; Konishi, G.; Klymchenko, A. S. *Sci. Rep.* **2016**, *6*, 18870. (b) Saito, Y.; Shinohara, Y.; Ishioroshi, S.; Suzuki, A.; Tanaka, M.; Saito, I. *Tetrahedron Lett.* **2011**, *52*, 2359−

DOI: 10.1021/acs.joc.7b00996
J. Org. Chem. 2017, 82, 6865−6873

2361. (c) Niko, Y.; Sugihara, H.; Suzuki, Y.; Kawamata, J.; Konishi, G. *J. Mater. Chem. B* **2015**, *3*, 184−190.
(8) Kim, Y. S.; Bae, S. Y.; Kim, K. H.; Lee, T. W.; Hur, J. A.; Hoang, M. H.; Cho, M. J.; Kim, S.-J.; Kim, Y.; Kim, M.; Lee, K.; Lee, S. J.; Choi, D. H. *Chem. Commun.* **2011**, *47*, 8907−8909.
(9) (a) Yang, X. H.; Giovenzana, T.; Felid, B.; Jabbour, G. E.; Sellinger, A. *J. Mater. Chem.* **2012**, *22*, 12689−12694. (b) Uchimura, M.; Watanabe, Y.; Araoka, F.; Watanabe, J.; Takezoe, H.; Konishi, G. *Adv. Mater.* **2010**, *22*, 4473−4478. (c) Thomas, K. R. J.; Kapoor, N.; Bolisetty, M. N. K. P.; Jou, J.-H.; Chen, Y.-L.; Jou, Y.-C. *J. Org. Chem.* **2012**, *77*, 3921−3932. (d) Kotchapradist, P.; Prachumrak, N.; Tarsang, R.; Jungsuttiwong, S.; Keawin, T.; Sudyoadsuk, T.; Promarak, V. *J. Mater. Chem. C* **2013**, *1*, 4916−4924. (e) Chercka, D.; Yoo, S.-J.; Baumgarten, M.; Kim, J.-J.; Müllen, K. *J. Mater. Chem. C* **2014**, *2*, 9083−9086.
(10) Niko, Y.; Sasaki, S.; Narushima, K.; Sharma, D. K.; Vacha, M.; Konishi, G. *J. Org. Chem.* **2015**, *80*, 10794−10805.
(11) Feng, X.; Tomiyasu, H.; Hu, J.-Y.; Wei, X.; Redshaw, C.; Elsegood, M. R. J.; Horsburgh, L.; Teat, S. J.; Yamato, T. *J. Org. Chem.* **2015**, *80*, 10973−10978.
(12) (a) Zöphel, L.; Beckmann, D.; Enkelmann, V.; Chercka, D.; Rieger, R.; Müllen, K. *Chem. Commun.* **2011**, *47*, 6960−6962. (b) Zöphel, L.; Enkelmann, V.; Rieger, R.; Müllen, K. *Org. Lett.* **2011**, *13*, 4506−4509.
(13) (a) Yamato, T.; Fuimoto, M.; Miyazawa, A.; Matsuo, K. *J. Chem. Soc., Perkin Trans. 1* **1997**, 1201−1208. (b) Gao, B.; Wang, M.; Cheng, Y.; Wang, L.; Jing, X.; Wang, F. *J. Am. Chem. Soc.* **2008**, *130*, 8297−8306. (c) Mateo-Alonso, A.; Kulisic, N.; Valenti, G.; Marcaccio, M.; Paolucci, F.; Prato, M. *Chem. - Asian J.* **2010**, *5*, 482−485. (d) Lucas, L. A.; DeLongchamp, D. M.; Richer, L. J.; Kline, R. J.; Fischer, D. A.; Kaafarani, B. R.; Jabbour, G. E. *Chem. Mater.* **2008**, *20*, 5743−5749. (e) Kohl, B.; Rominger, F.; Mastalerz, M. *Angew. Chem., Int. Ed.* **2015**, *54*, 6051−6056.
(14) (a) Mochida, K.; Kawasumi, K.; Segawa, Y.; Itami, K. *J. Am. Chem. Soc.* **2011**, *133*, 10716−10719. (b) Duong, H. M.; Bendikov, M.; Steiger, D.; Zhang, Q.; Sonmez, G.; Yamada, J.; Wudl, F. *Org. Lett.* **2003**, *5*, 4433−4436. (c) Xiao, J.; Duong, H. M.; Shi, W.; Ji, L.; Li, G.; Li, S.; Liu, X.-W.; Ma, J.; Wudl, F.; Zhang, Q. *Angew. Chem., Int. Ed.* **2012**, *51*, 6094−6098. (d) Baumgärtner, K.; Chincha, A. L. M.; Dreuw, A.; Rominger, F.; Mastalerz, M. *Angew. Chem., Int. Ed.* **2016**, *55*, 1−6.
(15) Zöphel, L.; Enkelmann, V.; Müllen, K. *Org. Lett.* **2013**, *15*, 804−807.
(16) (a) Keller, S. N.; Veltri, N. L.; Sutherland, T. C. *Org. Lett.* **2013**, *15*, 4798−4801. (b) Piotrowicz, M.; Zakrzewski, J.; Métivier, R.; Brosseau, A.; Makal, A.; Woźniak, K. *J. Org. Chem.* **2015**, *80*, 2573−2581.
(17) (a) Mei, J.; Leung, N. L. C.; Kwok, R. T. K.; Lam, J. W. Y.; Tang, B. Z. *Chem. Rev.* **2015**, *115*, 11718−11940. (b) Hong, Y.; Lam, J. W. Y.; Tang, B. Z. *Chem. Soc. Rev.* **2011**, *40*, 5361−5388.
(18) (a) Mei, J.; Hong, Y.; Lam, J. W. Y.; Qin, A.; Tang, Y.; Tang, B. Z. *Adv. Mater.* **2014**, *26*, 5429−5479. (b) Sasaki, S.; Konishi, G. *RSC Adv.* **2017**, *7*, 17403−17416. (c) Zhu, Q. H.; Ye, Z. W.; Yang, W. J.; Cai, X. T.; Tang, B. Z. *J. Org. Chem.* **2017**, *82*, 1096−1104. (d) Frath, D.; Benelhadj, K.; Munch, M.; Massue, J.; Ulrich, G. *J. Org. Chem.* **2016**, *81*, 9658−9668. (e) Mahendran, V.; Pasumpon, K.; Thimmarayaperumal, S.; Thilagar, P.; Shanmugam, S. *J. Org. Chem.* **2016**, *81*, 3597−3602. (f) Sasaki, S.; Niko, Y.; Igawa, K.; Konishi, G. *RSC Adv.* **2014**, *4*, 33474−33477.
(19) Sasaki, S.; Suzuki, S.; Sameera, W. M. C.; Igawa, K.; Morokuma, K.; Konishi, G. *J. Am. Chem. Soc.* **2016**, *138*, 8194−8206.
(20) (a) Bernardi, F.; Olivucci, M.; Robb, M. A. *Chem. Soc. Rev.* **1996**, *25*, 321−328. (b) Yarkony, D. R. *Acc. Chem. Res.* **1998**, *31*, 511−518.
(21) Harabuchi, Y.; Taketsugu, T.; Maeda, S. *Phys. Chem. Chem. Phys.* **2015**, *17*, 22561−22565.
(22) Hu, J.; Zhang, D.; Harris, F. W. *J. Org. Chem.* **2005**, *70*, 707−708.
(23) Mamada, M.; Perez-Bolivar, C.; Kumaki, D.; Esipenko, N. A.; Tokito, S.; Anzenbacher, P., Jr *Chem. - Eur. J.* **2014**, *20*, 11835−11846.
(24) Crawford, A. G.; Liu, Z.; Mkhalid, A. I.; Thibault, M.-H.; Schwarz, N.; Alcaraz, G.; Steffen, A.; Collings, J. C.; Batsanov, A. S.; Howard, J. A. K.; Marder, T. B. *Chem. - Eur. J.* **2012**, *18*, 5022−5035.
(25) Montalti, M.; Credi, A.; Prodi, L.; Gandolfi, M. T. *Handbook of Photochemistry*; Taylor & Francis: Boca Raton, 2006; pp 322.
(26) Ham, N. S.; Ruedenberg, K. *J. Chem. Phys.* **1956**, *25*, 13−26.
(27) Ferguson, J. *J. Chem. Phys.* **1958**, *28*, 765−768.
(28) Niko, Y.; Hiroshige, Y.; Kawauchi, S.; Konishi, G. *Tetrahedron* **2012**, *68*, 6177−6185.
(29) Niko, Y.; Kawauchi, S.; Otsu, S.; Tokumaru, K.; Konishi, G. *J. Org. Chem.* **2013**, *78*, 3196−3207.
(30) Spry, D. B.; Goun, A.; Bell, C. B., III; Fayer, M. D. *J. Chem. Phys.* **2006**, *125*, 114514.
(31) Filichev, V. V.; Astakhove, I. V.; Malakhov, A. D.; Korshun, V. A.; Pedersen, E. B. *Chem. - Eur. J.* **2008**, *14*, 9968−9980.
(32) Kalyanasundaram, K.; Thomas, J. K. *J. Am. Chem. Soc.* **1977**, *99*, 2039−2044.
(33) Sillen, A.; Engelborghs, Y. *Photochem. Photobiol.* **1998**, *67*, 475−486.
(34) Sasaki, S.; Igawa, K.; Konishi, G. *J. Mater. Chem. C* **2015**, *3*, 5940−5950.
(35) Hu, R.; Lager, E.; Aguilar, A. A.; Liu, J.; Lam, J. W. Y.; Sung, H. H. Y.; Williams, I. D.; Zhong, Y.; Wong, K. S.; Cabrera, E. P.; Tang, B. Z. *J. Phys. Chem. C* **2009**, *113*, 15845−15853.
(36) Niko, Y.; Kawauchi, S.; Konishi, G. *Chem. - Eur. J.* **2013**, *19*, 9760−9765.
(37) (a) Niko, Y.; Sasaki, S.; Kawauchi, S.; Tokumaru, K.; Konishi, G. *Chem. - Asian J.* **2014**, *9*, 1797−1807. (b) Niko, Y.; Cho, Y.; Kawauchi, S.; Konishi, G. *RSC Adv.* **2014**, *4*, 36480−36484.
(38) Katoh, R.; Suzuki, K.; Furube, A.; Kotani, M.; Tokumaru, K. *J. Phys. Chem. C* **2009**, *113*, 2961−2965.
(39) Oyamada, T.; Akiyama, S.; Yahiro, M.; Saigou, M.; Shiro, M.; Sasabe, H.; Adachi, C. *Chem. Phys. Lett.* **2006**, *421*, 295−299.
(40) Feng, Q.; Wang, M.; Dong, B.; Xu, C.; Zhao, J.; Zhang, H. *CrystEngComm* **2013**, *15*, 3623−3629.
(41) El-Assaad, T. H.; Auer, M.; Castaneda, R.; Hallal, K. M.; Jradi, F. M.; Mosca, L.; Khnayzer, R. S.; Patra, D.; Timofeeva, T. V.; Bredas, J.-L.; List-Kratochvil, E. J. W.; Wex, B.; Kaafarani, B. R. *J. Mater. Chem. C* **2016**, *4*, 3041−3058.
(42) Zhang, R.; Zhang, T.; Xu, L.; Han, F.; Zhao, Y.; Ni, Z. *J. Mol. Struct.* **2017**, *1127*, 237−246.
(43) Würthner, F.; Kaiser, T. E.; Saha-Möller, C. R. *Angew. Chem., Int. Ed.* **2011**, *50*, 3376−3410.
(44) Birks, J. B.; Kazzaz, A. A. *Proc. R. Soc. London, Ser. A* **1968**, *304*, 291−301.
(45) (a) Englman, R.; Jortner, J. *Mol. Phys.* **1970**, *18*, 145−164. (b) Siebrand, W. *J. Chem. Phys.* **1967**, *46*, 440−447.
(46) Reichardt, C. *Angew. Chem., Int. Ed. Engl.* **1979**, *18*, 98−110.
(47) (a) Mataga, N.; Kaifu, Y.; Koizumi, M. *Bull. Chem. Soc. Jpn.* **1955**, *28*, 690−691. (b) Lippert, E. L. *Organic Molecular Photophysics*; Wiley: New York, 1975.
(48) Cortes, J.; Heitele, H.; Jortner, J. *J. Phys. Chem.* **1994**, *98*, 2527−2536.
(49) Turro, N. J.; Ramamurthy, V.; Sciano, J. C. *Modern Molecular Photochemistry of Organic Molecules*; University Science Books: Sausalito, CA, 2010; pp 303−304.
(50) Blancafort, L. *ChemPhysChem* **2014**, *15*, 3166−3181.
(51) Zhang, T.; Jiang, Y.; Niu, Y.; Wang, D.; Peng, Q.; Shuai, Z. *J. Phys. Chem. A* **2014**, *118*, 9094−9108.
(52) Lakowicz, L. R. *Principles of Fluorescence Spectroscopy*, 3rd ed.; Springer Science+Business Media, LLC: New York, 2006; p 54.
(53) Sumi, K.; Niko, Y.; Tokumaru, K.; Konishi, G. *Chem. Commun.* **2013**, *49*, 3893−3895.
(54) Kortüm, G.; Braun, W.; Herzog, G. *Angew. Chem., Int. Ed. Engl.* **1963**, *2*, 333−304.

DOI: 10.1021/acs.joc.7b00996
J. Org. Chem. 2017, 82, 6865−6873